Int. J. Heat Mass Transfer. Vol. 32, No. 6, pp. 995–1006, 1989
Printed in Great Britain

0017–9310/89 $3.00 + 0.00
Pergamon Press plc

Unsteady diffusion mass transfer in a microencapsulated islet of Langerhans for a bioartificial pancreas

D. MORVAN† and M. Y. JAFFRIN‡

† U.M., C.N.R.S., 34, Institut de Mécanique des Fluides, 1 rue Honnorat, 13003 Marseille, France
‡ U.A., C.N.R.S., 858, Université de Technologie de Compiègne, Département Génie Biologique, B.P. 649, 60206 Compiègne Cedex, France

(*Received* 25 *April* 1988)

Abstract—A boundary element method (BEM) is used for the prediction of the kinetics of glucose and insulin transfer in a bioartificial pancreas model, constituted by a microencapsulated islet of Langerhans implanted in the peritoneal cavity. For each solute (glucose and insulin), the mass conservation equations inside and outside the microcapsule are reduced to a set of coupled integral equations which are solved using a collocation method. The insulin release localized on the islet of Langerhans is controlled by the local value of the glycemia. The analysis is made for a two-dimensional geometry with the following variations of the physical parameters: the microcapsule to islet size ratio $2 \leqslant R_m/R_i \leqslant 5$; the internal to external diffusion coefficient $0.1 \leqslant D_i/D_o \leqslant 1$; the dimensionless islet to arteriole distance $2 \leqslant Y_o/R_i \leqslant 7$.

1. INTRODUCTION

THE MICROENCAPSULATION of living cells represents a promising approach to bioartificial organs [1, 2]. The function of the microcapsule is to protect the cell from immune rejection. Therefore, its selective permeability must permit the diffusion of low molecular weight solutes while rejecting the antibodies and lymphocytes [3]. Various *in vivo* studies have shown that a single intraperitoneal transplant of encapsulated islets of Langerhans (the pancreatic cells which synthetize insulin) reversed the diabetic state for periods of up to one year [4]. These experimental results have proved the capacity of this bioartificial pancreas to keep the mean glycemia in the normal range during a long time, but they have not demonstrated that this system is able to avoid short hyperglycemia phases, which could appear after a meal. The aim therefore of this numerical model is to determine the glucose and insulin kinetics for a microencapsulated islet implanted in the peritoneal cavity near an arteriole during the short period (30 min) following an increase of blood glycemia. To approach this bioengineering mass transfer problem, which includes the transport of solutes through different media (inside and outside the microcapsule), we have used the subregion method, which consists of separating the computational domain into two parts and linking the two solutions by a set of transfer relations at the interface of the two adjacent subdomains. From a mathematical point of view, the solute mass conservation in each subregion is represented by a transient diffusion equation and a set of boundary and initial conditions.

This set of boundary value problems is solved using the boundary element method (BEM), which reduces each partial differential equation to an integral equation [5, 6]. The main advantage of this method is that it reduces the number of unknowns, which are now limited to the concentration and the mass flux of solute at the boundary. When this method is applied to a multi-region problem, the continuity of mass flux between adjacent boundaries is automatically taken into consideration. These two characteristics can explain the recent developments in applying this method to various physical problems, as in acoustics [7], fluid mechanics, solid mechanics or heat and mass transfer [8]. As a preliminary study, we have considered the case of a single unencapsulated islet implanted at various distances from the arteriole ($2 \leqslant Y_o/R_i \leqslant 7$). Then we have compared the results for a free islet and for a microencapsulated islet where the same medium is assumed to fill the inner and the outer microcapsule domains. Since the effect produced by a thin microcapsule upon the insulin release was found to be small, we have chosen to substitute for the microcapsule a microsphere and to study the influence of two physical parameters:

(a) the microsphere to islet radius ratio R_m/R_i ($2 \leqslant R_m/R_i \leqslant 5$);

(b) the diffusion coefficient ratio D_i/D_o ($0.1 \leqslant D_i/D_o \leqslant 1$) between the medium which constitutes the microsphere and the water which fills the peritoneal cavity.

For these different numerical tests the organization of the computations can be summarized as follows:

(a) evaluation of the glucose concentration field in each subdomain resulting from an instantaneous augmentation of the glycemia in the arteriole;

(b) calculation of the insulin release corresponding to the local increase of glycemia on the islet;

(c) evaluation of the insulin concentration field in

NOMENCLATURE

$\mathbf{A}^i, \mathbf{A}^o$	matrices representing the effect of the initial conditions inside and outside the microcapsule upon the integral equation
C	solute concentration
C^*	elementary solution of the transient diffusion equation
$\mathbf{D}_{gi}, \mathbf{D}_{go}$	glucose diffusion coefficient inside and outside the microcapsule
$\mathbf{D}_{ii}, \mathbf{D}_{io}$	insulin diffusion coefficient inside and outside the microcapsule
E_m	microcapsule thickness
G^n	$(n = 1, \ldots, 5)$ simple layer matrices representing the influence of the different parts of the boundary upon the integral equation
G_i, G_o	glucose concentration field inside and outside the microcapsule
H^n	$(n = 1, \ldots, 5)$ double layer matrices representing the influence of the different parts of the boundary upon the integral equation
$H_0(t)$	Heaviside distribution
$H_\Omega(M)$	characteristic function of the domain Ω
I_i, I_o	insulin concentration field inside and outside the microcapsule
k_g	glucose diffusion coefficient ratio between the inner and the outer microcapsular space: $\mathbf{D}_{gi}/\mathbf{D}_{go}$
k_i	insulin diffusion coefficient ratio between the inner and the outer microcapsular space: $\mathbf{D}_{ii}/\mathbf{D}_{io}$
n	unit outer vector normal on the boundary
Q	normal derivative of the solute concentration on the boundary
R_i	islet of Langerhans radius
R_m	microcapsule or microsphere radius
Sh_a	Sherwood number which characterizes the mass transfer through the arteriole wall
Sh_m	Sherwood number which characterizes the mass transfer through the microcapsule
t	time
Δt	time step
x, y	rectangular Cartesian coordinates
Y_o	distance between the centre of the islet and the arteriole wall.

Greek symbols

α	insulin to glucose diffusion ratio in an aqueous solution, $\mathbf{D}_{io}/\mathbf{D}_{go}$
$\Delta\Gamma$	mesh size
Γ_n	$(n = 1, \ldots, 5)$ different parts of the boundary
$\delta_t(0)$	temporal Dirac distribution with support $t = 0$
$\delta_x(\Gamma)$	spacial Dirac distribution with support Γ
$\delta'_{x,n}(\Gamma)$	normal derivative of $\delta_x(\Gamma)$ on Γ
$\delta_{x,t}(0,0)$	Dirac distribution with support $(M, t) = (0, 0)$
η	discretization parameter, $\Delta\Gamma/(k\Delta t)^{1/2}$
$\theta(M)$	internal angle subtended by boundary Γ at point M
Ω_i, Ω_o	inner and outer microcapsular domain.

the whole space and particularly the insulin flux which diffuses into the arteriole.

The mechanisms which participate in the insulin release can be regarded as a system constituted by two compartments in which the insulin is stored in a granular form [9, 10]. These two pools of insulin do not have equal capacities. The large pool represents the cytoplasmic pool containing mature insulin granules (98% of the total quantity of insulin stored), and the small pool represents the membrane-associated insulin granules that are immediately available for secretion [11]. Various *in vivo* and *in vitro* studies have established the stimulating action of glucose to insulin secretion [12]. The pancreatic response to a constant stimulation is characterized by a multiphasic pattern of insulin release which corresponds to the rapid liberation of the insulin granules stored in the cell membrane and the mobilization of the insulin produced in the Golgy apparatus and stored in the cytoplasm.

From a mathematical point of view, this behaviour can be modelled by a storage and signal limited model [13], which takes into account the fact that the insulin release arises from the combined effects of the insulin exchanges between the two compartments and the resulting balance of inhibitor and excitor substances.

2. GEOMETRY AND GOVERNING EQUATIONS

For simplicity, the solution of this mass transfer problem is limited to the two-dimensional case. The islet, the inner and the outer sides of the microcapsule and the arteriole wall are represented by their respective traces Γ_1, Γ_2, Γ_3 and Γ_5 in the computational plane. We have supposed that beyond a certain distance from the microcapsule the solute fields are uniform. Consequently the computational domain is artificially limited by a boundary Γ_4 (Fig. 1). The microcapsule divides the computational domain into

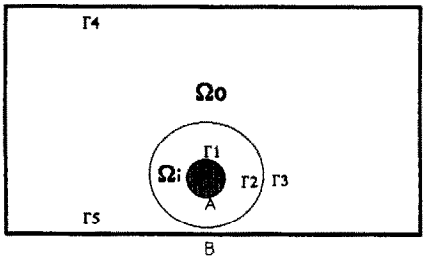

FIG. 1. Microencapsulated bioartificial pancreas: islet of Langerhans (Γ_1), microcapsule (Γ_2–Γ_3), arteriole wall (Γ_5).

two parts Ω_i, Ω_o which represent respectively the inner and the outer capsular spaces. In the absence of volumetric mass source and fluid flow, the mass conservation in each subdomain is described by the following transient diffusion equations:

for $M \in \Omega_i$, $t > 0$

$$\left[\frac{\partial G_i}{\partial t} - \mathbf{D}_{gi}\nabla^2 G_i\right](M,t) = 0 \tag{1a}$$

$$\left[\frac{\partial I_i}{\partial t} - \mathbf{D}_{ii}\nabla^2 I_i\right](M,t) = 0; \tag{1b}$$

for $M \in \Omega_o$, $t > 0$

$$\left[\frac{\partial G_o}{\partial t} - \mathbf{D}_{go}\nabla^2 G_o\right](M,t) = 0 \tag{1c}$$

$$\left[\frac{\partial I_o}{\partial t} - \mathbf{D}_{io}\nabla^2 I_o\right](M,t) = 0 \tag{1d}$$

with

$$\nabla^2 = \frac{\partial^2}{\partial x^2} + \frac{\partial^2}{\partial y^2} \quad \text{(Laplacian operator)}$$

where t is the time, $(\mathbf{D}_{gi}, \mathbf{D}_{go})$ and $(\mathbf{D}_{ii}, \mathbf{D}_{io})$ are the glucose and insulin diffusion coefficients in each subdomain Ω_i, Ω_o, and (G_i, G_o) and (I_i, I_o) are the glucose and insulin concentration fields inside and outside of the microcapsule. The reference scales are chosen as the islet radius R_i for the space variables and $R_i^2/\mathbf{D}_{go}$ for the time

$$t' = t\mathbf{D}_{go}/R_i^2, \quad x' = x/R_i, \quad y' = y/R_i.$$

The concentration of glucose is normalized with respect to G_a, the jump of glycemia imposed in the arteriole

$$G_i' = G_i/G_a, \quad G_o' = G_o/G_a.$$

The concentration of insulin is normalized with the insulin release observed in the steady state for a perfused pancreas stimulated by a jump of glycemia G_a [14]

$$I_i' = I_i/I_\infty(G_a), \quad I_o' = I_o/I_\infty(G_a)$$

$$I_\infty(G) = 0.05G^{10}/(8.875\times 10^{21} + 2.25\times 10^{15}G^3 + 3.5\times 10^6 G^7 + G^{10})$$

where G is given in mg dl^{-1} and I_∞ in μg cm^{-3}.

With the foregoing variables, the solute transport equations take the form (where the primes are omitted to simplify the expressions):

for $M \in \Omega_i$, $t > 0$

$$\left[\frac{\partial G_i}{\partial t} - k_g\nabla^2 G_i\right](M,t) = 0 \tag{2a}$$

$$\left[\frac{\partial I_i}{\partial t} - \alpha k_i\nabla^2 I_i\right](M,t) = 0; \tag{2b}$$

for $M \in \Omega_o$, $t > 0$

$$\left[\frac{\partial G_o}{\partial t} - \nabla^2 G_o\right](M,t) = 0 \tag{2c}$$

$$\left[\frac{\partial I_o}{\partial t} - \alpha\nabla^2 I_o\right](M,t) = 0 \tag{2d}$$

where we have introduced the following physical parameters:

(a) the insulin to glucose diffusion ratio in an aqueous solution (which constitutes the external domain Ω_o)

$$\alpha = \mathbf{D}_{io}/\mathbf{D}_{go};$$

(b) the glucose and insulin diffusion coefficient ratio between the inner and the outer capsule domain

$$k_g = \mathbf{D}_{gi}/\mathbf{D}_{go}, \quad k_i = \mathbf{D}_{ii}/\mathbf{D}_{io}.$$

The solution must verify an initial condition for $M \in \Omega_i \cup \Omega_o$ at $t = 0$

$$G_i = G_o = 0$$

$$I_i = I_o = 0$$

together with the following boundary conditions at $t > 0$ (where n is the unit outer vector normal to the boundary):

for $M \in \Gamma_1$, the islet is impermeable to glucose and the concentration of insulin on the membrane cell I_{iL} is fixed by the insulin release model

$$\frac{\partial G_i}{\partial n} = 0 \tag{3a}$$

$$I_i = I_{iL}; \tag{3b}$$

for $M \in \Gamma_2$ and Γ_3, the mass flux is continuous at the interface of the two computational domains Ω_i, Ω_o

$$\frac{\partial G_o}{\partial n} = -k_g\frac{\partial G_i}{\partial n} \tag{3c}$$

$$\frac{\partial I_o}{\partial n} = -k_i\frac{\partial I_i}{\partial n}. \tag{3d}$$

When the interface Γ_2, Γ_3 represents a thin microcapsule, the solute concentration fields are discontinuous through it and the jump between the two solutions is defined by the following relations:

$$\frac{1}{Sh_{mg}}\frac{\partial G_o}{\partial n} = [G_i - G_o] \tag{3e}$$

$$\frac{1}{Sh_{mi}}\frac{\partial I_o}{\partial n} = [I_i - I_o] \tag{3f}$$

where Sh_{mg} and Sh_{mi} are the Sherwood numbers which characterized the glucose and insulin mass transfer respectively through the microcapsular membrane. For a thin membrane, the solute concentration profile can be considered as linear: therefore the Sherwood numbers are given by

$$Sh_{mg} = Sh_{mi} = R_i/E_m$$

where E_m is the capsule thickness.

The particular case where the islet is located in a single microsphere without a microcapsule can be described by the limit $E_m \to 0$; in that case $Sh_{mg} = Sh_{mi} \to \infty$ and the solute concentration becomes continuous at the interface

$$G_i = G_o \tag{3g}$$

$$I_i = I_o. \tag{3h}$$

For $M \in \Gamma_4$, beyond the boundary Γ_4, the solute concentration fields are uniform

$$\frac{\partial G_o}{\partial n} = 0 \tag{3i}$$

$$\frac{\partial I_o}{\partial n} = 0. \tag{3j}$$

for $M \in \Gamma_5$, the concentration of glucose and the mass flux of insulin are fixed on the arteriole wall

$$G_o = 1 \quad \text{for} \quad 0 < t < T_1$$

$$G_o = 0 \quad \text{for} \quad T_1 < t$$

$$\frac{\partial I_o}{\partial n} = Sh_{ai}[I_a - I_o]$$

where I_a is the bulk insulin concentration in the arteriole and Sh_{ai} is the Sherwood number which characterizes the insulin transfer through the arteriole wall.

3. BOUNDARY ELEMENT FORMULATION AND NUMERICAL RESOLUTION

3.1. *Boundary element formulation*

The partial differential equations which compose system (2) can be written in the general form

$$\left[\frac{\partial C}{\partial t} - k\nabla^2 C\right](M,t) = 0 \tag{4}$$

where C is a function (or, more generally, a distribution), compactly supported in Ω, a bounded domain of space R^2 (with a regular boundary Γ). The initial and boundary conditions associated with this general problem can be summarized as follows:

for $M \in \Omega$, $t = 0$

$$C(M,0) = C_0(M); \tag{5a}$$

for $M \in \Gamma_a$, $t > 0$ (Dirichlet)

$$\operatorname{Tr} C(M,t) = C_a(M,t); \tag{5b}$$

for $M \in \Gamma_b$, $t > 0$ (Neumann)

$$\operatorname{Tr} \partial_n C(M,t) = Q_b(M,t); \tag{5c}$$

for $M \in \Gamma_c$, $t > 0$ (Robin)

$$(A \operatorname{Tr} C + B \operatorname{Tr} \partial_n C) = F_c(M,t). \tag{5d}$$

The values of C and $\partial_n C$ on Γ are defined as the limits

$$\operatorname{Tr} C(P) = \lim_{M \in \Omega \to P \in \Gamma} C(M) \tag{6a}$$

$$\operatorname{Tr} \partial_n C(P) = \lim_{M \in \Omega \to P \in \Gamma} \partial_n C(M). \tag{6b}$$

We now consider the distribution C^+ defined as the prolongation of C by zero in the whole space R^2

$$C^+(M,t) = H_o(t) H_\Omega(M) V(M,t) \tag{7}$$

where $H_o(t)$ is the Heaviside distribution ($H_o(t) = 0$ if $t < 0$ and $H_o(t) = 1$ if $t > 0$) and $H_\Omega(M)$ is the characteristic function of the domain Ω ($H_\Omega(M) = 0$ if $M \in R^2 - \bar{\Omega}$ and $H_\Omega(M) = 1$ if $M \in \Omega$). This function is not differentiable in the vicinity of Γ: its derivatives must be taken in the distribution sense [15]. Therefore, C^+ satisfies the following partial differential equation in Ω as well as in $R^2 - \bar{\Omega}$ (in the distribution sense):

$$\left[\frac{\partial C^+}{\partial t} - k\nabla^2 C^+\right](M,t) = C_0(M)\delta_t(0) + k\left[\operatorname{Tr}\frac{\partial C}{\partial n}\delta_x(\Gamma) + \operatorname{Tr} C\delta'_{x,n}(\Gamma)\right](M,t). \tag{8}$$

In equation (8) $\delta_t(0)$ and $\delta_x(\Gamma)$ are respectively the Dirac distributions with support $t = 0$ and Γ. Let C^* be the fundamental solution (Green function) of the transient diffusion equation, defined by

$$\left[\frac{\partial C^*}{\partial t} - k\nabla^2 C^*\right](M,t) = \delta_{x,t}(0,0) \tag{9a}$$

$$C^*(M,t) = \frac{H_o(t)}{4\pi k t}\exp\left[-\frac{|OM|^2}{4kt}\right] \tag{9b}$$

where $\delta_{x,t}(0,0)$ is the Dirac distribution with support $(x,t) = (0,0)$. Taking the specific properties of the convolution product into account, the solution C^+, in whole space R^2, is given by the following integral expression:

$$\theta(M)C^+(M,t) = \left\{C_0(M)\delta_t(0) + k\left[\operatorname{Tr}\frac{\partial C}{\partial n}\delta_x(\Gamma) + \operatorname{Tr} C\delta'_{x,n}(\Gamma)\right](M,t)\right\} * C^*(M,t) \tag{10}$$

where $\theta(M) = 1$ for $M \in \Omega$, $\theta(M) = \varphi/2\pi$ for $M \in \Gamma$, $\theta(M) = 0$ for $M \in R^2 - \bar{\Omega}$. $*$ denotes the convolution product; φ is the angle subtended by Γ at M, if M is a regular point on Γ: $\varphi = \pi$.

Finally, the development of the convolution product permits us to say that the solution verifies an integral equation

$$\theta(M)C^+(M,t) = \int_\Omega C_0(P)C^*(PM,t)\,\mathrm{d}P + k\int_\Gamma\int_0^t [Q^+(P,\tau)C^*(PM,t-\tau) - C^+(P,\tau)Q^*(PM,t-\tau)]\,\mathrm{d}\tau\,\mathrm{d}P \quad (11)$$

where

$$Q^+(P,\tau) = \mathrm{Tr}\,\partial_n C(P,\tau) \text{ and } C^+(P,\tau) = \mathrm{Tr}\,C(P,\tau)$$
$$Q^*(P,\tau) = \partial_n C^*(P,\tau) \text{ for } P\in\Gamma.$$

The integral equation (11) is the classical BEM formulation for the resolution of the general diffusion problem (equations (4) and (5)).

3.2. *Numerical resolution*

The resolution of the integral equation system, resulting from the applications of the BEM formulation (11) to the set of transient diffusion equations (2), is performed numerically using a collocation method. This discretization method includes a piecewise constant approximation in time and a usual finite element decomposition in space (Fig. 2) [5, 15]. To obtain a good and convergent approximation, the mesh size $\Delta\Gamma$ and the time step Δt must satisfy a consistency condition [16]. For a bilinear finite element this relation is

$$\eta = \frac{\Delta\Gamma}{\sqrt{(k\Delta t)}} \leqslant 1. \quad (12)$$

The time marching is carried out by choosing at each time step the initial concentration field as the solution evaluated just before. The discretization of each integral equation includes the evaluation of time integrals, which are performed analytically, and also space integrations which are approximated using the standard Gaussian quadrature. An exception is made for those in which the boundary element contains a collocation node, since in these cases the integrals become singular. The integral is then divided into two parts—one regular, which is approximated numerically as previously; the other, which contains the logarithmic singularity, is computed analytically [5, 15].

After performing all these integrations, the set of boundary integral equations, which represents the mass transfer problem for one solute inside the two subregions Ω_i and Ω_o, can be written as the following algebraic system:

$$[H^1H^2]\begin{Bmatrix} C^m_{\Gamma_1} \\ C^m_{\Gamma_2}\end{Bmatrix} = [G^1G^2]\begin{Bmatrix} \partial_n C^m_{\Gamma_1} \\ \partial_n C^m_{\Gamma_2}\end{Bmatrix} + [A^i]\{C^{m-1}_{\Omega_i}\} \quad (13a)$$

$$[H^3H^4H^5]\begin{Bmatrix} C^m_{\Gamma_3} \\ C^m_{\Gamma_4} \\ C^m_{\Gamma_5}\end{Bmatrix} = [G^3G^4G^5]\begin{Bmatrix} \partial_n C^m_{\Gamma_3} \\ \partial_n C^m_{\Gamma_4} \\ \partial_n C^m_{\Gamma_5}\end{Bmatrix} + [A^o]\{C^{m-1}_{\Omega_o}\}, \quad (13b)$$

where $\{C_{\Gamma_i}, \partial_n C_{\Gamma_i}\}^m$ are the solute (glucose or insulin) concentration and mass flux on the different parts Γ_i $(i = 1,\ldots,5)$ of the boundary at time t_m and $\{C_{\Omega_i}, C_{\Omega_o}\}^{m-1}$ are the solute concentration fields inside each subregion Ω_i and Ω_o at time t_{m-1}. Introducing for each solute its specific boundary conditions (3), the whole problem is reduced to the resolution of the two following algebraic systems:

$$\begin{bmatrix} H^1_g & H^2_g & -G^2_g & 0 & 0 \\ 0 & H^3_g & k_g G^3_g + \dfrac{k_g}{Sh_{mg}} H^3_g & H^4_g & -G^5_g \end{bmatrix} \times \begin{Bmatrix} G_{\Gamma_1} \\ G_{\Gamma_2} \\ \partial_n G_{\Gamma_2} \\ G_{\Gamma_4} \\ \partial_n G_{\Gamma_5} \end{Bmatrix} = \begin{Bmatrix} [A^i_g]\{G^{m-1}_{\Omega_i}\} \\ [A^o_g]\{G^{m-1}_{\Omega_o}\} \\ -[H^5_g]\{1\} \end{Bmatrix} \quad (14a)$$

$$\begin{bmatrix} -G^1_i & H^2_i & -G^2_i & 0 & 0 \\ 0 & H^3_i & k_i G^3_i + \dfrac{k_i}{Sh_{mi}} H^3_i & H^4_i & H^5_i + Sh_{ai} G^5_i \end{bmatrix} \times \begin{Bmatrix} \partial_n I_{\Gamma_1} \\ I_{\Gamma_2} \\ \partial_n I_{\Gamma_2} \\ I_{\Gamma_4} \\ I_{\Gamma_5} \end{Bmatrix} = \begin{Bmatrix} [A^i_i]\{I^{m-1}_{\Omega_i}\} \\ -[H^1_i]\{I_{iL}\} \\ [A^o_i]\{I^{m-1}_{\Omega_o}\} \\ +Sh_{ai}[G^5_i]\{I_{iL}\} \end{Bmatrix}. \quad (14b)$$

Resolving the two linear systems (14), we obtain the concentrations and mass flux of glucose and insulin on the boundary at each time step. Then integral expressions (11) permit the evaluation at the same time the concentration fields inside the two subdomains Ω_i and Ω_o.

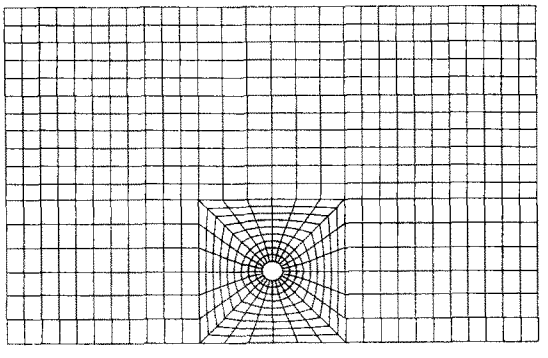

FIG. 2. Finite element mesh.

4. NUMERICAL RESULTS

As a preliminary study, we have considered a single unencapsulated islet implanted in the peritoneal cavity

which is assumed to be filled with water ($k_g = k_i = k = 1$). Various islet to arteriole wall distances Y_o have been considered to evaluate the effect of the geometrical parameter Y_o/R_i on the glucose and insulin kinetics ($2 \leqslant Y_o/R_i \leqslant 7$).

The concentration of glucose in the arteriole is imposed as a square signal with an amplitude $G_a = 210$ mg dl^{-1} during $T_1 = 20$ min—this input condition induces a steady state insulin release value $I_\infty = 0.032$ μg cm^{-3}. The islet radius considered is $R_i = 50$ μm; the glucose and insulin diffusion coefficients in an aqueous solution are: $\mathbf{D}_g = 9.09 \times 10^{-6}$ cm^2 s^{-1} and $\mathbf{D}_i = 2.00 \times 10^{-6}$ cm^2 s^{-1}, which give $\alpha = 0.22$ and $T_{ref} = R_i^2/\mathbf{D}_g = 2.75$ s.

The Sherwood number which characterizes the mass transfer through the arteriole wall is defined as the laminar flow in a rectangular duct: $Sh_a = 7.6$ [17]. Figures 3–5 represent the evolution with time of the glucose and insulin concentrations on the islet (point A on Fig. 1) and on the arteriole wall (point B on Fig. 1). These different curves show that an increase of the dimensionless distance Y_o/R_i increases the delay of the glucose signal on the islet (Fig. 3) and decreases the insulin release, on both the islet (Fig. 4) and the arteriole wall (Fig. 5). When the ratio Y_o/R_i increases from 2 to 7, the mean concentration of insulin during the stimulation phase ($0 \leqslant T/T_{ref} \leqslant 430$) decreases on the islet (point A) from 0.32 to 0.22 and on the arteriole

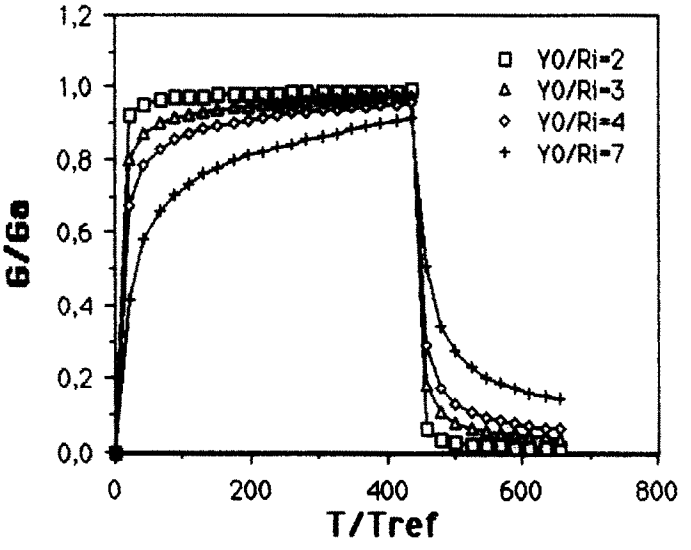

FIG. 3. Concentration of glucose on the islet (point A) when the islet to arteriole wall distance (Y_o) varies ($G_a = 210$ mg dl^{-1}, $T_{ref} = 2.75$ s).

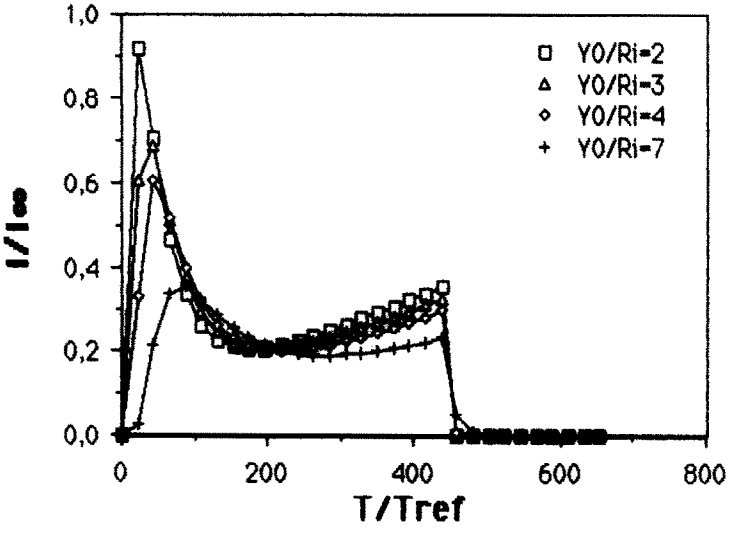

FIG. 4. Concentration of insulin on the islet (point A) when the islet to arteriole wall distance (Y_o) varies ($I_\infty = 0.032$ μg cm^{-3}, $T_{ref} = 2.75$ s).

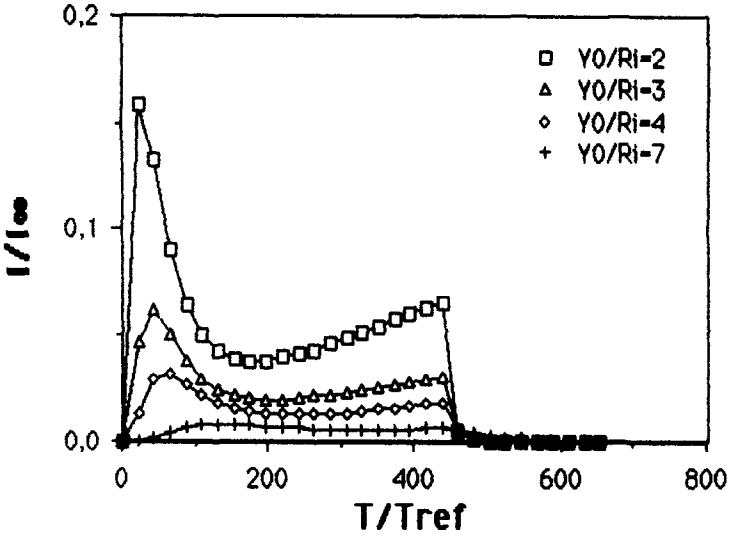

FIG. 5. Concentration of insulin on the arteriole wall (point B) when the islet to arteriole wall distance (Y_0) varies ($I_\infty = 0.032\ \mu g\ cm^{-3}$, $T_{ref} = 2.75$ s).

wall (point B) from 0.06 to 0.005. This modification of the insulin release is also detectable in Fig. 6, which represents the instantaneous insulin concentration field at different times $T/T_{ref} = 43$, 86, 215 and 430. On these different plots we can observe the rapid dilution of the insulin from the islet membrane to the arteriole wall and the shifting of the maximum insulin release value from $T/T_{ref} = 43$ to 86 when the islet leaves the arteriole wall. In each numerical experiment the insulin release signal is characterized by a biphasic pattern.

(1) A rapid and short release phase which corresponds to the instantaneous liberation of insulin granules stored in the islet membrane. Comparing Figs. 3 and 4, we can observe that the amplitude of this early phase (Fig. 4) decreases as the glucose stimulation signal (Fig. 3) is delayed.

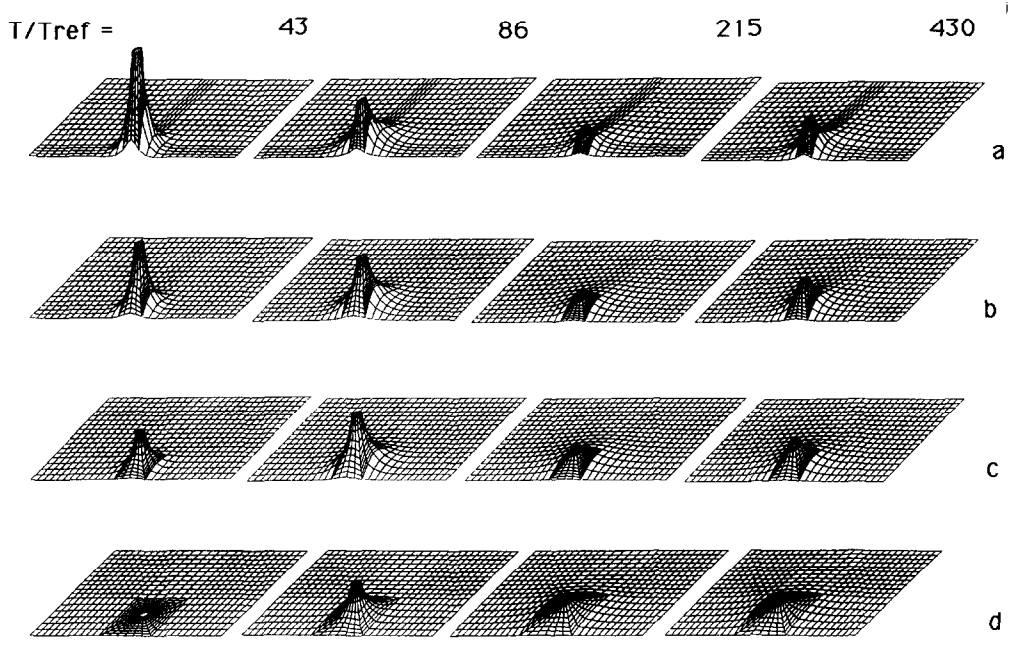

FIG. 6. Insulin concentration field during the stimulation of a single unencapsulated islet when the islet to arteriole wall distance varies ($T_{ref} = 2.75$ s): (a) $Y_0/R_i = 2$; (b) 3; (c) 4; (d) 7.

(2) A more progressive release phase which is produced by the mobilization of insulin granules produced in the Golgy apparatus and stored in the cytoplasm.

We then carried out a numerical test for a microencapsulated islet in the same stimulation conditions. The microcapsule is defined by its dimensions and its physical properties:

(a) the dimensionless membrane thickness $E_m/R_i = 0.1$ ($Sh_{mg} = Sh_{mi} = 10$);

(b) the capsule to islet radius ratio $R_m/R_i = 3$;

(c) the diffusion coefficient ratio of a solute through the membrane and in an aqueous solution $k_m = \mathbf{D}_m/\mathbf{D} = 0.3$ (this is the common value encountered for a hydrogel which constitutes the microcapsular membrane) [18].

To analyse the specific effect produced by the microencapsulation upon the insulin release, we have assumed that the inner microcapsular space, like the outer one, was filled with water; we have also in this case therefore $k_g = k_i = 1$. The results illustrated in Figs. 7 and 8 show that both glucose and insulin kinetics were not affected by the presence of the microcapsule. The microcapsular membrane seems to represent a very thin resistance for the glucose and insulin transfer between the islet and the arteriole wall. The foregoing result is not consistent with a previous

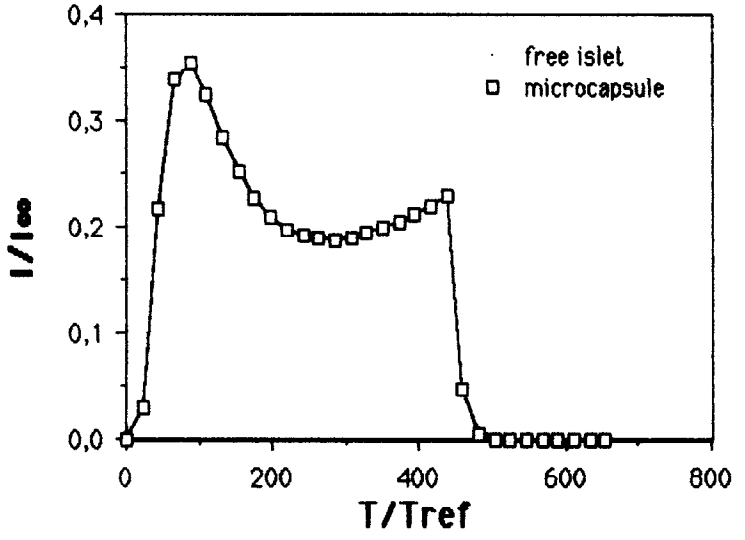

FIG. 7. Concentration of insulin on the islet (point A) for a microencapsulated and a free islet ($I_\infty = 0.032$ μg cm^{-3}, $T_{ref} = 2.75$ s).

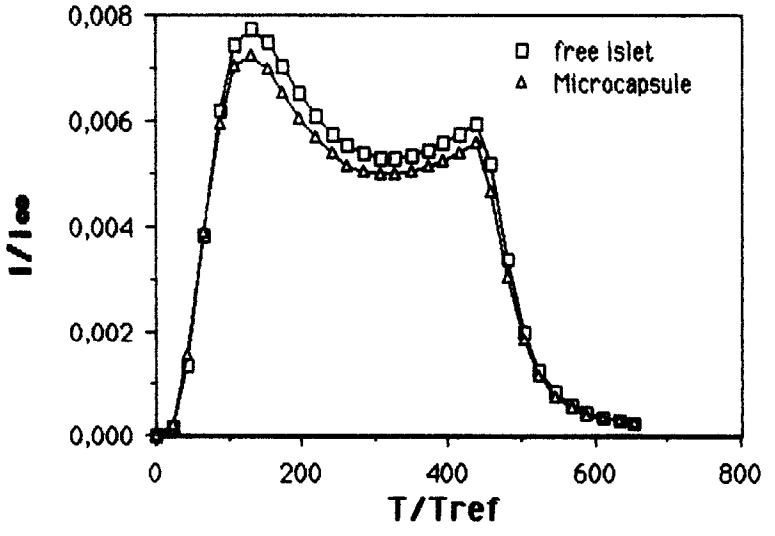

FIG. 8. Concentration of insulin on the arteriole wall (point B) for a microencapsulated and a free islet ($I_\infty = 0.032$ μg cm^{-3}, $T_{ref} = 2.75$ s).

experimental *in vitro* study [19], which demonstrated that the insulin release ratio between a microencapsulated and a free islet was approximately equal to 4. The apparent contradiction between these two results is probably caused by the supplementary resistance produced by the existence of a different medium inside the microcapsule. We can therefore neglect the effect of the microcapsule, regarding the islet as located inside a microsphere characterized by two parameters:

(a) the microsphere to islet radius ratio R_m/R_i;
(b) the diffusion coefficient ratios k_g and k_i.

Figures 9–12 represent the evolution in time of the insulin concentration obtained on the islet (point A: Figs. 9 and 11) and on the arteriole wall (point B: Figs. 10 and 12) for two sets of numerical tests

$$Y_o/R_i = 7, \quad k_g = k_i = k = 0.3,$$
$$R_m/R_i = 2, 3, 4 \text{ and } 5$$
$$Y_o/R_i = 7, \quad R_m/R_i = 3,$$
$$k_g = k_i = k = 0.1, 0.2, 0.3, 0.5 \text{ and } 1.$$

Figures 9 and 11 show that a reduction of the microsphere to islet ratio or the microsphere resistance

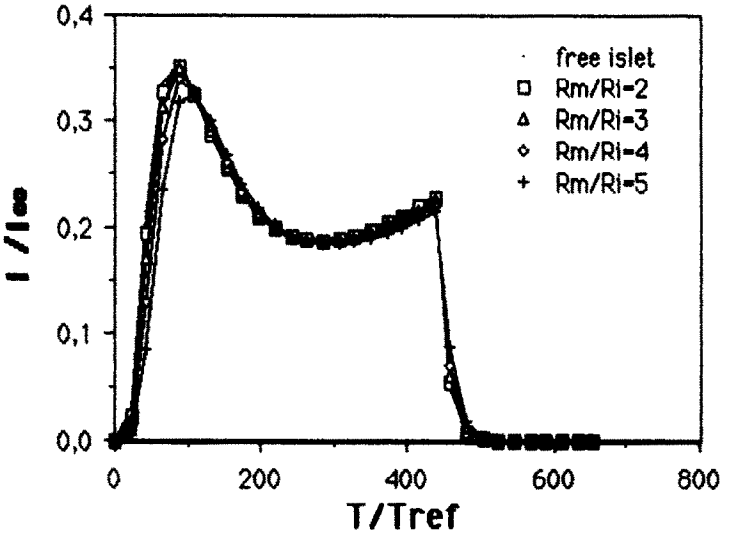

FIG. 9. Concentration of insulin on the islet (point A) when the microsphere to islet radius ratio R_m/R_i varies ($R_i = 50$ μm, $I_\infty = 0.032$ μg cm^{-3}, $T_{ref} = 2.75$ s).

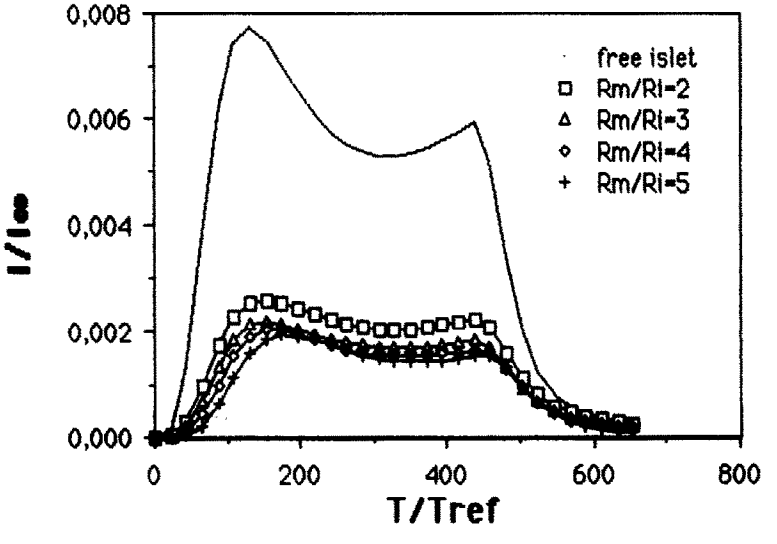

FIG. 10. Concentration of insulin on the arteriole wall (point B) when the microsphere to islet radius ratio R_m/R_i varies ($R_i = 50$ μm, $I_\infty = 0.032$ μg cm^{-3}, $T_{ref} = 2.75$ s).

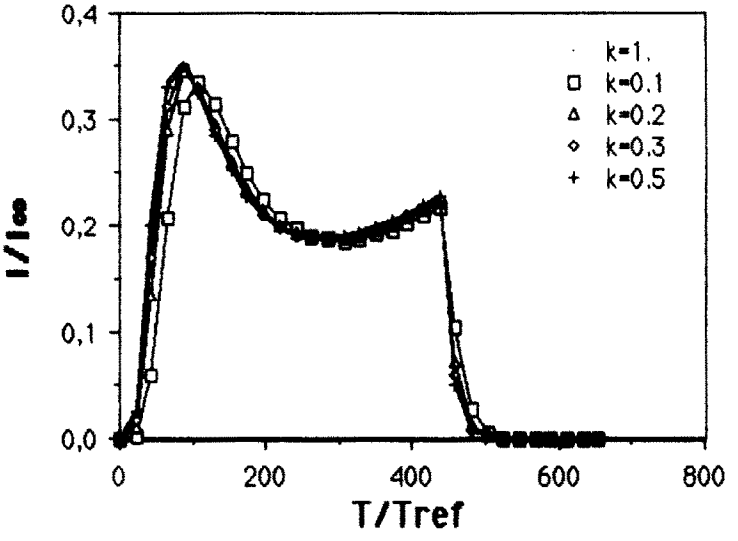

FIG. 11. Concentration of insulin on the islet (point A) when the diffusivity ratio $k_g = k_i = k$ varies ($I_\infty = 0.032\ \mu g\ cm^{-3}$, $T_{ref} = 2.75$ s).

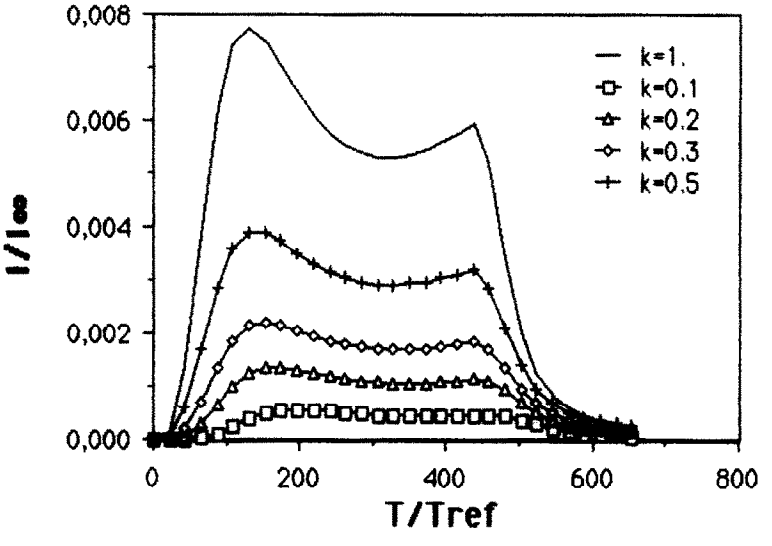

FIG. 12. Concentration of insulin on the arteriole wall (point B) when the diffusivity ratio $k_g = k_i = k$ varies ($I_\infty = 0.032\ \mu g\ cm^{-3}$, $T_{ref} = 2.75$ s).

does not affect the insulin release located on the islet. Nevertheless, Figs. 10 and 12 show that these modifications appreciably affect the insulin which diffuses through the arteriole wall:

(a) when R_m/R_i is reduced from 5 to 2 the mean insulin concentration during the stimulation phase ($0 \leqslant T/T_{ref} \leqslant 430$) increases from 0.197 to 0.210 on the islet and from 1.24×10^{-3} to 1.86×10^{-3} on the arteriole wall;

(b) when k increases from 0.1 to 0.5 the same mean insulin concentration increases from 0.198 to 0.210 on the islet and from 3.6×10^{-4} to 2.71×10^{-3} on the arteriole wall.

5. CONCLUSION

This paper has described a numerical study of the mass transfer processes in a bioartificial pancreas model. The mathematical problem has been solved using the BEM associated with the subregions formulation. Various numerical experiments have been carried out to test the effect of different physical parameters upon the glucose and insulin kinetics during their transfer between an implanted islet of Langerhans and an arteriole.

We have found that the insulin quantity diffusing through the arteriole wall depends on the resistance to diffusion of the medium located between the islet

and the arteriole wall. While the kinetics of glucose do not seem to be affected by a small modification to the transfer conditions between the islet and the arteriole, the kinetics of insulin are extremely sensitive to such conditions. The insulin available for diffusion in the vascular system is considerably reduced as the islet to arteriole wall distance increases, or if the diffusion coefficient between the islet and the arteriole decreases. This behaviour presents a problem for the use of microencapsulated islets as a bioartificial pancreas. Since it is impossible to predict the location of each islet implanted in the peritoneal cavity, the number of islets necessary for the normalization of glycemia in diabetics and their distance from an arteriole cannot be determined with precision and it will be impossible to predict the insulin release in blood produced by this technique. In this respect, therefore, the bioartificial pancreas placed as an arteriovenous shunt [20, 21], which offers better control of the insulin release, seems a more promising technique.

REFERENCES

1. F. Lim, Microencapsulated hepatocytes as a potential bioartificial liver, *Artificial Organs* **5,** 304–306 (1981).
2. F. Lim and A. M. Sun, Microencapsulated islets as bioartificial endocrine pancreas, *Science* **210,** 908–910 (1980).
3. G. Reach, Bioartificial pancreas, present state and future prospects, *Biomed. Biochim. Acta* **43,** 569–576 (1984).
4. M. F. A. Goosen, G. M. O'Shea, H. M. Gharapetian, S. Chou and A. M. Sun, Optimization of microcapsules as a bioartificial pancreas, *Biotech. Bioengng* **27,** 146–150 (1985).
5. L. C. Wrobel, Potential and viscous flow problems using the boundary element method. Ph.D. Thesis, University of Southampton (1981).
6. C. A. Brebbia and L. C. Wrobel, Steady and unsteady potential problems using the boundary element method. In *Recent Advances in Numerical Methods in Fluids* (Edited by C. Taylor and K. Morgan), Chap. 1, pp. 1–25. Pineridge Press, Swansea (1980).
7. P. J. T. Filippi, Layer potentials and acoustic diffraction, *J. Sound Vibr.* **54,** 473–500 (1977).
8. C. A. Brebbia, Boundary element methods in engineering. *Proc. 4th Int. Sem. on Boundary Element Methods in Engineering*, Southampton. Springer, Berlin (1982).
9. G. M. Grodsky, D. Curry, H. Landhal and L. L. Bennett, Further studies on the dynamic aspects of insulin release *in vitro* with evidence for a two-compartmental storage system, *Acta Diabet. Lat.* **6,** 554–579 (1969).
10. D. L. Curry, L. L. Bennett and G. M. Grodsky, Dynamics of insulin secretion by the perfused rat pancreas, *Endocrinology* **83,** 572–584 (1968).
11. L. A. Campfield and D. C. Blocker, Stimulation of the autonomic neural control of insulin secretion, *Comp. Biol. Med.* **9,** 191–203 (1979).
12. J. E. Gerich, M. A. Charles and G. M. Grodsky, Characterization of the effects of arginine and glucose on glucagon and insulin release from the perfused rat pancreas, *J. Clin. Invest.* **54,** 833–841 (1974).
13. H. Landahl and G. M. Grodsky, Comparison of models of insulin release, *Bull. Math. Biol.* **44,** 399–409 (1982).
14. G. M. Grodsky, A threshold distribution hypothesis for packet storage of insulin and its mathematical modeling, *J. Clin. Invest.* **51,** 2047–2059 (1972).
15. J. L. M. Fernandes and H. L. G. Pina, Unsteady heat conduction using the boundary element method. In *Boundary Element Methods in Engineering* (Edited by C. A. Brebbia), pp. 156–170 (1982).
16. A. Chaudouet, Three-dimensional transient thermoelastic analyses by the B.I.E. method, *Int. J. Numer. Meth. Engng* **24,** 25–45 (1987).
17. L. Wolf and S. Zaltzman, Optimum geometry for artificial kidney dializers. In *The Artificial Kidney* (Edited by P. L. Dedrick, K. B. Bischoff and E. F. Leonard), Chem. Engng Prog. Symp. Ser. 84, pp. 104–111 (1968).
18. N. A. Peppas and C. T. Reinhart, Solute diffusion in swollen membranes. Part 1. A new theory, *J. Membrane Sci.* **43,** 275–287 (1983).
19. D. Chicheportiche and G. Reach, *In vitro* kinetics of insulin release by microencapsulated islets: effect of the size of the microcapsules. *Diabetologia* No. 31, 54–57 (1988).
20. W. L. Chick, A. A. Like, V. Lauris, P. M. Galletti, P. D. Richardson, G. Panol, T. W. Mix and C. K. Colton, A hybrid artificial pancreas, *Trans. ASAIO* **21,** 8–14 (1975).
21. G. Reach, M. Y. Jaffrin and J. F. Desjeux, A U-shaped bioartificial pancreas with rapid glucose–insulin kinetics, *Diabetes* **33,** 752–760 (1984).

TRANSFERT DE MASSE PAR DIFFUSION INSTATIONNAIRE DANS UN ILOT MICROENCAPSULE POUR UN PANCREAS BIOARTIFICIEL

Résumé—Une méthode d'éléments finis de frontière est utilisée pour la prédiction des transferts de glucose et d'insuline dans un modèle de pancréas bioartificiel. Le transfert de soluté est assuré par diffusion instationnaire, les concentrations à l'intérieur et à l'extérieur de la microcapsule sont données par deux équations intégrales de frontière qui sont résolues par une méthode de collocation. La libération d'insuline localisée sur l'îlot de Langerhans est contrôlée par la valeur locale de la glycémie. L'analyse des transferts est développée pour une géométrie bidimensionnelle lorsque les paramètres physiques varient : rapport de taille microcapsule/îlot $2 \leqslant R_m/R_i \leqslant 5$; rapport de diffusivité milieu interne et externe à la microcapsule $0.1 \leqslant D_i/D_o \leqslant 1$; distance adimensionnée îlot–artériole $2 \leqslant Y_o/R_i \leqslant 7$.

INSTATIONÄRER MASSENTRANSPORT DURCH DIFFUSION IN EINER MIKROGEKAPSELTEN LANGERHANS'SCHEN INSEL EINES KÜNSTLICHEN PANKREAS

Zusammenfassung—Zur Beschreibung des Glukose- und Insulin-Transports in einem künstlichen Pankreas-Modell, das aus einer mikrogekapselten Langerhans'schen Insel besteht, die in einem Hohlraum des Bauchfells implantiert ist, wird eine Grenzflächenmethode verwendet. Die Massenerhaltungsgleichungen für jeden gelösten Stoff (Glukose und Insulin) innerhalb und außerhalb der Mikrokapsel werden zu einem Satz gekoppelter Integralgleichungen reduziert, die mit einem Kollokationsverfahren gelöst werden. Die Insulinabgabe der Langerhans'schen Inseln wird durch den örtlichen Glukosegehalt geregelt. Es wird eine zweidimensionale Geometrie untersucht. Die folgenden physikalischen Parameter werden variiert: das Verhältnis der Größe von Mikrokapsel zu Langerhans'scher Insel $2 \leqslant R_m/R_i \leqslant 5$; das Verhältnis von innerem zu äußerem Diffusionskoeffizienten $0{,}1 \leqslant D_i/D_o \leqslant 1$; der dimensionslose Abstand zwischen Langerhans'scher Insel und Arteriole $2 \leqslant Y_o/R_i \leqslant 7$.

НЕСТАЦИОНАРНЫЙ ДИФФУЗИОННЫЙ МАССОПЕРЕНОС В ЗАКЛЮЧЕННОЙ В МИКРОКАПСУЛУ ЧАСТИЦЕ ЛАНГЕРХАНСА В ИСКУССТВЕННОЙ ПОДЖЕЛУДОЧНОЙ ЖЕЛЕЗЕ

Аннотация—Методом граничных элементов рассчитывается кинетика переноса глюкозы и инсулина в модели искусственной поджелудочной железы, образованной заключенной в микрокапсулу частицей Лангерханса, помещенной в перитоническую полость. Уравнения сохранения массы внутри и вне микрокапсулы для каждого растворенного вещества (глюкозы и инсулина) сводятся к системе связанных интегральных уравнений, решаемых методом коллокаций. Поток инсулина, локализованный на чистице Лангерханса, регулируется местным уровнем гликемии. Проведен анализ двумерной геометрии для следующих диапазонов физических параметров: отношение размеров капсулы и частицы $2 \leqslant R_m/R_i \leqslant 5$; отношение коэффициентов внутренней и внешей диффузии $0{,}1 \leqslant D_i/D_o \leqslant 1$; обезразмеренная по размеру частицы артериальная длина $2 \leqslant Y_o/R_i \leqslant 7$.